

Sulindac imprinted mungbean starch/PVA biomaterial films as a transdermal drug delivery patch

Hye-Yeong Tak^{a,1}, Yeon-Hum Yun^{b,1}, Chang-Moon Lee^{c,1}, Soon-Do Yoon^{a,*}

^a Department of Chemical and Biomolecular Engineering, Chonnam National University, Yeosu 59626, Republic of Korea

^b Department of Energy & Resources Engineering, Chonnam National University, Gwangju 61186, South Korea

^c Department of Biomedical Engineering, Chonnam National University, Yeosu 59626, Republic of Korea



ARTICLE INFO

Keywords:

Biomaterial films
Sulindac
Physical properties
Recognition ability
Drug release property

ABSTRACT

In this work, biodegradable biomaterial films for sulindac (SLD) recognition are synthesized from mungbean starch (MBS), PVA, and plasticizers by using UV irradiation process and casting methods. The optimal UV irradiation time for the preparation of SLD imprinted biomaterials films was about 30 min. Mechanical properties, recognition ability, and SLD release property for prepared films were investigated. From the results of recognition ability, we verified that these SLD imprinted biomaterial films have the binding site for SLD. The release properties of SLD was examined with the change of pH and temperature. The results indicate that the SLD release in pH 10.0 was higher than in pH 4.0. SLD release was also evaluated using an artificial skin. Results of the artificial skin test verified that SLD was released constantly for 20 days.

1. Introduction

Due to recent developments in science and technology over the last few decades, synthetic polymers based on petroleum have been increasingly produced worldwide each year. Convenience, safety, low price, and good aesthetic qualities are the most important factors that contribute to the rapid growth in the use of plastics for various purposes such as biomedical materials, packaging, transportation, industry and agriculture in both rural and urban areas. However, indiscriminate use of synthetic polymers and mismanagement have caused serious environmental problems (Nair & Laurencin, 2007; Tian, Tang, Zhuang, Chen, & Jing, 2012), including pollution and global warming due to increased problem of waste disposal and land filling. In addition, CO₂ and dioxins are released when they are burned and incinerated. Therefore, there has been increasing interest in the removal and minimization of environmental problems caused by non-degradable synthetic polymers. Many studies have been carried out to develop eco-friendly biodegradable polymers as a replacement of synthetic polymer materials. Due to their functionalities, such eco-friendly biodegradable polymers, have applications in various fields (Sadanand, Rajini, Rajulu, & Satyanarayana, 2016; Tian, Yan, Rajulu, Xiang, & Luo, 2017; Wu et al., 2016).

Biodegradable polymers can be degraded fast by microbes. It has been reported that microbes can degrade most organic and inorganic

materials, including alginate, lignin, chitosan, starch, gelatine, cellulose and hemicelluloses (Imre & Pukánszky, 2013; Yu, Dean, & Li, 2006). Of various renewable sources of biodegradable polymers, starch is one of the most promising natural biodegradable polymer because of its inherent biodegradability, abundance, and renewability. It is composed of a mixture of two substances, an essentially linear amylose (10–30%) and a highly branched amylopectin (70–90%). The amylose content of some starches is higher than 40% (Fu et al., 2018; Mikus et al., 2014; Yun & Yoon, 2010).

Starch-based biopolymers are very attractive and practical biodegradable biomaterials because of their low material cost and ability to be processed with conventional plastic processing or a simple apparatus. Starch-based biodegradable materials for general and functional applications are being actively developed due to oil shortage and growing interest in environmental problems associated with extensive use of petrochemical-derived polymers (Ali et al., 2018; Robles, Salaberria, Herrera, Fernandes, & Labidi, 2016; Sanuja, Agalya, & Umopathy, 2015; Wang et al., 2016). However, they have limitations in applications because they are extremely brittle with inherently poor water resistance properties. Thus, various studies and methods such as blending starch with petroleum-derived materials, adding functional plasticizers, crosslinking by using chemical agents, heat treatment, or photo-irradiation, and using nanocomposites have been tried to improve their physical properties and applicability (Aydm & Ilberg, 2016;

* Corresponding author.

E-mail address: yunsd03@jnu.ac.kr (S.-D. Yoon).

¹ These authors contributed equally to this work.

Byun, Park, Lim, & Yoon, 2011; Delville, Joly, Dole, & Bliard, 2002; Jose, Al-Harhi, AlMáadeed, Dakua, & De, 2015; Liu et al., 2012; Ma, Chang, Yu, & Lu, 2008; Reddy & Yang, 2010; Xie, Pollet, Halley, & Avérous, 2013).

Among them, photo-irradiation is a very useful and simple cross-linking method due to low cost and high efficiency. Especially, ultraviolet (UV) irradiation curing as a crosslinking method has advantages in the following: 1) the curing speed is fast, which is beneficial to get high quality products and improve preparation efficiency; 2) energy consumption is low, and 3) the curing temperature is low. UV irradiated materials are known to have excellent performance. In addition, UV irradiation process is environmentally friendly. Thus, UV irradiation process has attracted great attention (Cieśla, Abramowska, Boguski, & Drewnik, 2017; Niazi & Broekhuis, 2015; Xiao & Hao, 2010; Zhang, Windall, & Boyd, 2002; Zhou et al., 2009). UV curing is carried out by a photosensitivity of photosensitizers, an excited-state molecule formed under UV light, then decomposing it into free radicals. These unsaturated organic compounds can be achieved by polymerization, grafting, and cross-linking (Lv et al., 2018). Follain, Joly, Dole, and Bliard, (2005) and Delville et al. (2002) reported that mechanical and water resistance properties of starch-based films adding sodium benzoate (SB) and benzophenone (BP) as photosensitizers were improved by the UV curing process. In addition, the evaluation of physical properties and thermal analysis for starch-based materials using various photosensitizers such as SB, organic acid, and moisture was reported by Niazi and Broekhuis, (2015). In this study, we try to prepare starch-based biopolymer using UV irradiation process by moisture.

Starch-based biopolymer is able to apply as functional biomaterials such as wound dressings, carrier for drug delivery, and transdermal drug delivery patch. Of these application fields, Transdermal drug delivery system (TDDS) patch is an attractive replacement method for oral delivery of drugs. It is also an alternative to hypodermic injection (Brown, Martin, Jones, & Akomeah, 2006; Kwak, Jeong, & Suh, 2011; Lam & Gambari, 2014; Prausnitz & Langer, 2008). Through TDDS, dosage can be designed to deliver a therapeutically effective amount of drug across the skin. TDDS has the following advantages: (1) superior patient compliance; (2) avoidance of first pass metabolism, and (3) potential for decreased side effects resulting from the ability to give lower doses with high efficacy (Asbill et al., 2000). A variety of biocompatible polymeric materials such as poly(2-hydroxyethyl methacrylate), polyvinylpyrrolidone, poly(methyl methacrylate), poly(vinyl alcohol), poly(acrylic acid), polyacrylamide, poly(ethylene-co-vinylacetate), polyethylene glycol, poly(methacrylic acid), polylactides (PLA), polyglycolides (PGA), poly(lactide-co-glycolides) (PLGA), poly-anhydrides, polyorthoesters, proteins (silk, collagen, gelatin, β -casein, zein, and albumin), and carbohydrates (polysaccharides such as chitosan, chitin, alginate, pullulan, starch, and heparin) have been used as transdermal patches for TDDS (Banerjee, Chattopadhyay, Ghosh, Datta, & Veer, 2014). However, starch-based biomaterials for application in transdermal patch have not been reported yet.

Sulindac (SLD) was used as the imprinted (target) drug in this study. SLD is one of the early nonsteroidal anti-inflammatory drugs (NSAIDs) known to inhibit activities of cyclooxygenases. However, it is known that digestive disorders, stomach ulcers, headache, pancreatitis, cholestasis, itching, sensitivity to light, tinnitus, hair loss, high blood pressure, edema, palpitations, hematological disorders, painful urination, proteinuria and hematuria occurs as side effects (Maciążek-Jurczyk & Sułkowska, 2015). Therefore, it is necessary to control the release of SLD to remove or decrease these side effects of drugs while increasing the efficacy and duration of the therapeutic effect.

The objective of this study was to prepare SLD imprinted MBS/PVA biomaterials for application in TDDS using UV irradiation process and to evaluate physical properties of MBS/PVA biomaterial films prepared with UV irradiation time, the degree of recognition of SLD for quantitative release of drug, and drug release under different pH and temperature conditions. The degree of SLD release was also investigated

using an artificial skin test.

2. Materials and methods

2.1. Materials

Mungbean starch (MBS) was obtained from Chungwonfood Korea, Inc. Polyvinyl alcohol (PVA), sulindac (SLD), reagent grade glycerol (GL), citric acid (CA), ascorbic acid (AsA), and dimethyl sulfoxide (DMSO) were purchased from Sigma-Aldrich Chemical Company, Inc. (Milwaukee, WI, USA). PVA was 99% hydrolyzed with a molecular weight average of 89,000–98,000. Ethanol and standard buffer solution (pH = 4.01, pH = 7.0, and pH = 10) were obtained from Duksan (Pharmaceutical Co., Ltd., Korea). Distilled deionized water (DW) was used in all experiments.

2.2. Preparation of SLD imprinted MBS/PVA biomaterial films

SLD imprinted MBS/PVA biomaterials films were prepared by a simple casting method and UV curing process. First, PVA solution was prepared by dissolving PVA in hot water (90 °C). MBS and plasticizers (GL, CA, or AsA) were then mixed with water using a kitchen-aid mixer (Anymix, Hyun-woo Star, Seoul, Korea) for 20 min. PVA solution and mixed MBS/plasticizers were kept at 95 °C for 10 min. Then, the mixture was blended to form homogeneously gel-like solution with a mechanical stirrer (600 rpm) at room temperature for 60 min. After dissolving SLD (0.2 g) as the target drug in ethanol (20 mL), SLD solution was added dropwise for 10 min for uniform recognition on gel-like solution during blending. The composition for the preparation of SLD imprinted MBS/PVA biomaterial films is listed in Table 1. Bubbles as by-product of preparation were removed using an aspirator. The gel-like solution prepared was then poured on to a pre-warmed (60 °C) teflon mold (250 × 250 × 1.0 mm). Water was evaporated from the molds in a ventilated oven at 60 °C for 24 h. These prepared biomaterial films were then irradiated for 10, 20, 30, 40, 50, and 60 min using a UV lamp (OSRAM ULTRA-VITALUX, 300 W) at atmospheric pressure. After UV irradiation process, these films were conditioned again at 25 °C with RH 55% for one week.

The characterization of UV irradiated MBS/PVA biomaterial films with/without SLD was carried out using a surface analysis and Fourier transform infrared spectrophotometry (FT-IR) analysis. Surfaces of UV irradiated MBS/PVA biomaterial films with/without SLD were examined using a scanning electron microscopy (SEM) (S-4700, Hitachi, Tokyo, Japan), at an acceleration voltage of 5 kV. FT-IR (IRPrestige-21, Shimadzu, Japan) spectra of MBS/PVA biomaterial films with UV irradiation time were recorded on a FT-IR spectroscopy. These samples were thoroughly dried in a vacuum oven at 50 °C, and 15 scans were taken for each sample.

2.3. Tensile strength (TS) and elongation at break (%E)

Mechanical properties such as tensile strength (TS) and elongation

Table 1
The composition for the preparation of MBS/PVA biomaterial films.

Sample name	MBS (g)	PVA (g)	GL (wt%)	CA (wt%)	AsA (wt%)	SLD (g)	DW (g)
MBS-P	5.0	5.0	–	–	–	–	100
MBS-P-SLD	5.0	5.0	–	–	–	0.2	100
MBS-PGL4	5.0	5.0	40	–	–	–	100
MBS-PGL4-SLD	5.0	5.0	40	–	–	0.2	100
MBS-PCA4	5.0	5.0	–	40	–	–	100
MBS-PCA4-SLD	5.0	5.0	–	40	–	0.2	100
MBS-PAsA4	5.0	5.0	–	–	40	–	100
MBS-PAsA4-SLD	5.0	5.0	–	–	40	0.2	100

at break (%E) were investigated for each film using an Instron 6012 testing machine. Five dumbbell shaped specimens (ASTM D-412) were cut out of each film. The thickness of each film was measured at five places along the test length using a mechanical scanner (Digital thickness gauge "Mitutoyo" Tokyo, Japan) at 15 random positions around the film. The average thickness of specimens was 0.120 ± 0.005 mm. Gauge length and grip distance were both 55.0 mm. The crosshead speed was at 20 mm/min, and the load cell capacity was 250 kg_f. All tests were conducted at 25 °C with RH 52.0%.

2.4. Swelling behavior and solubility

Swelling behavior (SB) and solubility (S) of these prepared films were evaluated using the following method. First, dried films were immersed in distilled water at room temperature (25 °C) for 24 h to reach equilibrium. After that the weight of the swollen films was measured. SB of film was calculated using the following Eq. (1):

$$SB = \frac{W_e - W_0}{W_0} \quad (1)$$

where W_e is the weight of the film at the adsorbing equilibrium, and W_0 is the first dry weight of the film. These swollen films were dried again at 60 °C for 24 h. The solubility (S) of each film was calculated with the following Eq. (2):

$$S = \frac{W_0 - W_d}{W_d} \quad (2)$$

where W_0 is the first dry weight of the film and W_d is the dry weight of the swollen film.

2.5. Gel fraction

Gel fraction of MBS/PVA biomaterial films prepared with UV irradiation time was conducted as described by [Zhai, Yoshii, and Kume, \(2003\)](#). Briefly, MBS/PVA biomaterial films were placed into stainless net of about 200 mesh and immersed in DMSO for 72 h at room temperature to extract the soluble part. After washing several times with distilled water and methyl alcohol, samples were dried to constant weight at 50 °C. Gel fraction was calculated with the following Eq. (3):

$$\text{Gel fraction (\%)} = \frac{W_g}{W_0} \times 100 \quad (3)$$

where W_g is the weight of dry gel after extraction and W_0 is the initial weight of dry biomaterial films.

2.6. Recognition properties for SLD imprinted MBS/PVA biomaterial films

To evaluate recognition properties of prepared biomaterials films, we carried out Soxhlet extraction for SLD imprinted into biomaterials films. The removal of SLD was conducted in ethanol as a good solvent of SLD. Biomaterial films were then cleaned with DW and ethanol alternately until SLD was not detected by UV–vis spectrophotometer (OPTIZEN 2120UV, Neogen, Co., Ltd, Korea). These biomaterial films with SLD removed were dried in a vacuum oven at 50 °C for 12 h. Binding isotherms were calculated by adding a fixed amount of 0.1 g of biomaterial films into 45 mL vial containing 30 mL of different initial concentrations of SLD (0.10–1.50 mmol/L). These vials were agitated in an isothermal shaker at 200 rpm and for 12 h at 25 °C until equilibrium was reached. Aqueous samples were then taken from these solutions and concentrations of SLD were analyzed. In addition, the binding isotherm for non-imprinted SLD biomaterial films was examined by the same procedure to verify the effect on recognition for SLD. The adsorbed amount (Q) of SLD bound to the imprinted biomaterials films was calculated by the following Eq. (4):

$$Q (\mu\text{mol/g}) = \frac{(C_i - C_e) \cdot V}{W} \quad (4)$$

where C_i and C_e are concentrations of SLD (mmol/L) measured at the initial and equilibrium, respectively. V is the volume of the solution (L) and W is the mass of the dry imprinted biomaterial films used (g).

To estimate the binding affinity of the biomaterial films for SLD, Scatchard plot analysis was carried out. The Scatchard equation is shown below (5):

$$Q / [\text{Template}] = \frac{(Q_{\text{max}} - Q)}{K_D} \quad (5)$$

where Q is the amount of SLD bound to biomaterial films at equilibrium, Q_{max} is the apparent maximum number of binding sites, $[\text{Templates}]$ is the free SLD concentration at equilibrium and K_D is the equilibrium dissociation constant of binding site.

2.7. Release properties of SLD

The influence of pH and temperature of SLD imprinted MBS/PVA biomaterial films on release properties was examined to evaluate its applicability as a TDDS patch. Prepared biomaterial films (0.10 g) were immersed in pH 4.0, 7.0, or 10.0 solution of 100 mL in flasks. These flasks were then incubated at 25, 37, or, 45 °C on a shaking (80 rpm) incubator (VS-8480SF, Vision, Scientific Co., Korea). At predetermined time point, 2 mL of the solution from release medium was taken and the released SLD was analyzed by UV–vis spectrophotometer at 327.3 nm. The percentage of cumulative amount of released SLD was calculated from the standard calibration curve prepared previously. In addition, the possibility as TDDS patch was verified by drug release test using an artificial skin (NeodermR-ED, Tego Science, Inc. Korea) at 36.5 °C and RH of 60.0%.

3. Results and discussion

3.1. Effects of UV irradiation process on MBS/PVA biomaterial films

It is necessary to crosslink eco-friendly biodegradable biomaterials based on natural polymers because of their water-soluble properties. In addition, the crosslinking process plays an important role in expanding their application fields such as biomedical, environmental, food, and separation technology. Generally, natural polymer based biomaterials are crosslinked using chemical agents, heat curing, and gamma, electron beam, or UV irradiation ([Yun, Lee, Kim, & Yoon, 2017](#)). In this study, MBS/PVA biomaterial films without the addition of photosensitizer were synthesized using UV irradiation process. The optimum irradiation time was confirmed.

[Fig. 1](#) shows results of the effect of UV irradiation on TS, %E, SB, and S for the prepared MBS/PVA biomaterial films without addition of plasticizers. With an increase in UV irradiation time, TS increased whereas %E rapidly decreased ([Fig. 1a](#)). These results indicated that TS and %E values of prepared biomaterials films were changed due to deformation such as yellowing and discoloration when irradiation time was increased to more than 30 min. When materials are exposed to excessive heat or light, mechanical properties of biomaterials are enhanced. However, such treatment can reduce their applicability as biomedical materials and engineering because of the increase in brittle properties. [Fig. 1b](#) shows SB and S of prepared biomaterial films with different UV irradiation time. Results showed that SB and S decreased with increasing UV irradiation time. Such results are attributed to crosslinking caused by UV irradiation. In addition, the decrease in SB and S implies an increasing in the degree of crosslinking because SB and S are closely related to the degree of crosslinking. These results verified that physical properties of MBS/PVA biomaterial films were improved by UV irradiation due to increase of crosslinking. In addition, these results showed that SB and S drastically decreased until 30 min after UV

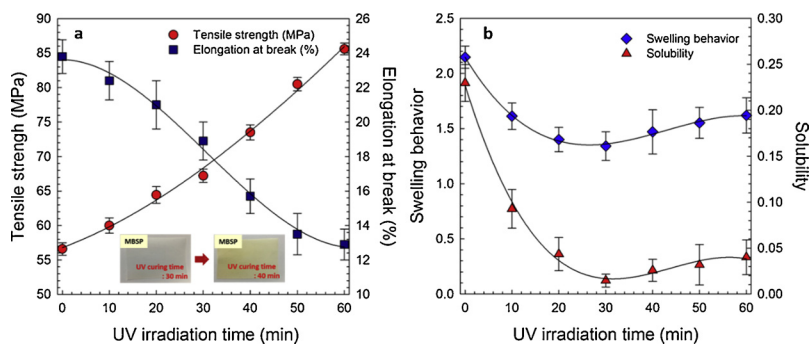


Fig. 1. Physical properties of MBS/PVA biomaterial films with UV irradiation times. (a) Tensile strength (TS) and elongation at break (%E) of biomaterial films with UV irradiation times, (b) Swelling behavior (SB) and solubility (S) of biomaterial films with UV curing times.

irradiation. However, a slight increase of SB and S occurred after 30 min. This might be due to the fact that crosslinking was not carried out or molecules of short length and polymer chains degraded by UV irradiation were dissolved in water. Based on these results, we synthesized sulindac (SLD) imprinted MBS/PVA biomaterial films using UV irradiation time of about 30 min.

Gel fraction is an important factor to determine the degree of crosslinking in hydrogels or films (Noori, Kokabi, & Hassan, 2018). To verify the degree of crosslinking, we performed gel fraction test of MBS/PVA biomaterial films prepared with different UV irradiation time. Gel fraction of the prepared MBS/PVA biomaterial films are shown in Fig. 2a. With increasing UV irradiation time, gel fraction was increased drastically until 30 min. It was then slightly decreased when UV irradiation time was more than 40 min. These results indicate that interactions between components of biomaterial films are improved by UV irradiation. These results also verified that gel fraction was decreased when UV irradiation was increased to be more than 40 min.

It has been reported that the degree of crosslinking combination is possible by FT-IR analysis (Elizondo, Sobral, & Menegalli, 2009). Results of FT-IR analysis of MBS/PVA biomaterial films prepared with different UV irradiation time are shown in Fig. 2b. Peaks appeared at 842.6 and 932.5 cm^{-1} due to $-\text{C}-\text{O}-\text{C}-$ ring vibration in granular starch (Das et al., 2010) and 999.5 cm^{-1} due to $-\text{CH}$ bending of vinyl groups. Peaks observed at 1153.5 and 1084.5 cm^{-1} are characteristic of anhydroglucose ring found in starch. Peaks at 1324.6 – 1328.1 and 1424.7 cm^{-1} were assigned to deformation vibration of $-\text{CH}_2$ in $-\text{CH}_2\text{OH}$. The broad band at 3284.9 cm^{-1} as asymmetry and symmetry stretching was attributed to hydrogen bonded hydroxyl groups ($-\text{OH}$). This band provides an important evidence for the existence of hydrogen bonding in the polymer network. We identified an increase of transmittance of the broad band at 3284.9 cm^{-1} with an increase in UV irradiation time. These results indicate that hydrogen bonding force among MBS and PVA hydroxyl groups and crosslinking combination are increased by UV irradiation (Kim, Park, Rhim, & Lee, 2005; Yu et al.,

2018). When compared to MBSP and UV-irradiated MBSP, a slight shift occurred for peaks at 1324.6 – 1328.1 cm^{-1} . The result indicates that the shift of the peak was due to difference in their mode of vibrations depending on their crosslinking by UV irradiation.

3.2. Physical properties of SLD imprinted MBS/PVA biomaterials films

Biomaterial films based natural polymers such as starch, chitosan, gelatin, and cellulose have been prepared using various plasticizers because of their high rigidity, low workability, and weak water resistance properties. Therefore, we prepared SLD imprinted MBS/PVA biomaterial films using GL, CA, and AsA as plasticizers, and evaluated their mechanical properties such as tensile strength (TS) and elongation at break (%E) for application as transdermal drug delivery patch. In addition, recognition properties of MBS/PVA biomaterial films imprinted the target drug were investigated to quantitatively evaluate degree of loading for the target drug. The extraction process of the target drug was carried out to evaluate recognition properties.

Tensile strength (TS) and elongation at break (%E) as mechanical properties of SLD imprinted MBS/PVA biomaterial films with/without addition of 40 wt% GL, CA, and AsA as plasticizers before/after the extraction of SLD as target drug are shown in Table 2. TS of non-added plasticizers biomaterial films was higher than that of biomaterial films added with plasticizers whereas %E of biomaterial films added plasticizers was higher than that of biomaterial films without added plasticizers. These results revealed that the flexibility of biomaterial films could be improved by adding plasticizers. %E is known to play an important role in the flexibility for application in various fields. The difference in %E value with various types of plasticizers is in the following increasing order: MBSPCA4 > MBSPGL4 > MBSPAsA4. When mechanical properties of non-imprinted SLD were compared to those of SLD imprinted MBS/PVA biomaterial films, similar mechanical properties were found although the removal of SLD was conducted using an extraction process.

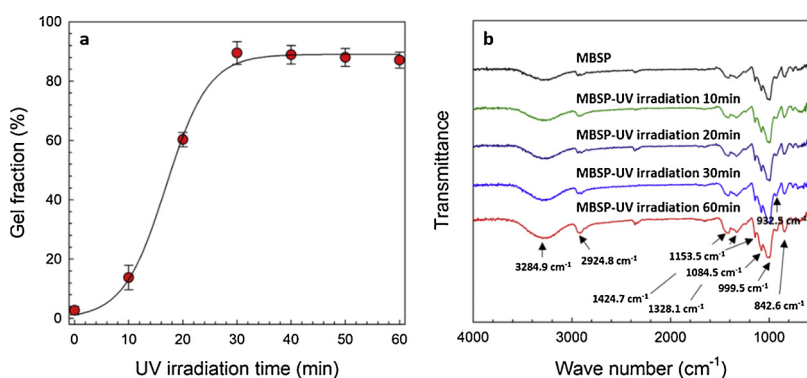


Fig. 2. (a) Gel fraction of MBS/PVA biomaterial films with UV irradiation times. (b) FT-IR spectra of MBS/PVA biomaterial films with UV irradiation times.

Table 2
Mechanical properties of SLD imprinted MBS/PVA biomaterial films.

Sample name	Tensile strength (MPa)		Elongation at break (%)	
	Before extraction	After extraction	Before extraction	After extraction
MBSP	67.2 ± 1.10	–	18.9 ± 1.09	–
MBSP–SLD	71.4 ± 1.51	73.8 ± 1.21	19.2 ± 1.43	16.2 ± 1.01
MBSPGL4	19.7 ± 2.01	–	100.1 ± 1.67	–
MBSPGL4–SLD	22.4 ± 1.41	20.6 ± 1.25	95.6 ± 1.23	85.4 ± 1.30
MBSPCA4	48.7 ± 1.51	–	121.5 ± 1.12	–
MBSPCA4–SLD	53.1 ± 1.23	47.2 ± 1.46	115.7 ± 2.01	100.9 ± 1.87
MBSPAsA4	39.8 ± 1.55	–	99.7 ± 1.47	–
MBSPAsA4–SLD	43.8 ± 1.12	40.8 ± 1.51	87.4 ± 1.36	79.3 ± 1.42

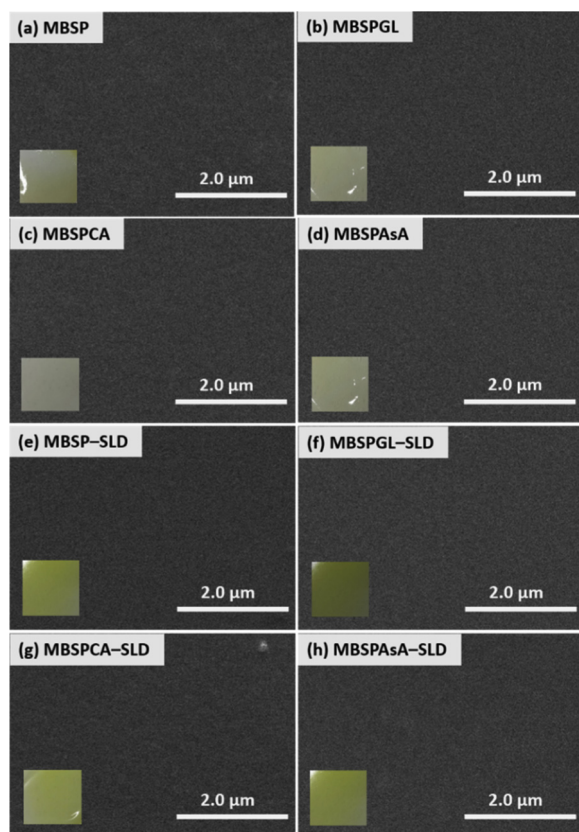


Fig. 3. SEM images of surfaces of UV irradiated MBS/PVA biomaterial films. (a) MBS/PVA biomaterial films without imprinted SLD. (b) GL-added MBS/PVA biomaterial films without imprinted SLD. (c) CA-added MBS/PVA biomaterial films without imprinted SLD. (d) AsA-added MBS/PVA biomaterial films without imprinted SLD. (e) SLD imprinted MBS/PVA biomaterial films. (f) GL-added MBS/PVA biomaterial films with imprinted SLD. (g) CA-added MBS/PVA biomaterial films with imprinted SLD. (h) AsA-added MBS/PVA biomaterial films with imprinted SLD.

Fig. 3 shows SEM images of surfaces of UV irradiated MBS/PVA biomaterial films added with 40 wt% plasticizers (GL, CA, and AsA) with/without the recognition of SLD. Surfaces of these biomaterial films added with plasticizers without imprinted SLD appeared relatively homogeneous and smooth. For SLD imprinted biomaterial films, yellow biomaterial films were formed. This is because SLD is a yellow crystalline compound. SEM images of surfaces of SLD imprinted biomaterial films added with plasticizers showed no noticeable agglomeration, cracks, debonding, or voids.

3.3. Recognition properties of SLD imprinted MBS/PVA biomaterial films

Recognition property is an important factor in quantitative analysis

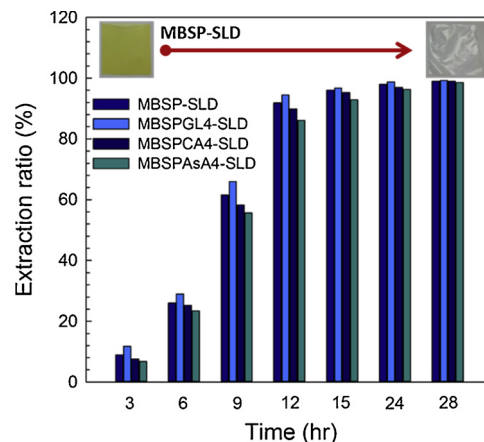


Fig. 4. Extraction ratio (%) of SLD into SLD imprinted MBS/PVA biomaterial films.

of optimal dose or release control of target drug as well as the expansion of application fields such as coating material for biosensor and selective separation of target material. In this study, recognition properties for SLD imprinted MBS/PVA biomaterial films were investigated by binding isotherm and Scatchard plot analysis. These analyses used re-binding of SLD on biomaterial films in which SLD was extracted as a target drug. Fig. 4 shows extraction ratio (%) with extraction time (hr) for SLD imprinted MBS/PVA biomaterials films with/without the addition of plasticizers (GL, CA, and AsA). The extraction of SLD was calculated from the extraction ratio (%) of SLD imprinted biomaterial films (0.1 g) including SLD. SLD as a tare drug was extracted above 98.5% in about 28 h, although there was a difference in extraction ratio depending on the type of plasticizers added.

Fig. 5 shows binding isotherm and Scatchard plot for SLD on UV irradiated SLD imprinted MBS/PVA biomaterial films. Results of binding isotherm for UV irradiated SLD imprinted MBS/PVA biomaterial films with/without the addition of GL, CA, and AsA are shown in Fig. 5a. The adsorbed amount (Q) was slowly increased with increasing concentration of SLD in the initial solution. The Q of SLD on imprinted biomaterial films was higher than that of non-imprinted biomaterial films. The increase in Q is ascribed to the influence of molecular recognition for the target drug. These results verified that Q values differed among types of plasticizers. These results revealed that CA-added SLD imprinted biomaterial film was superior to GL-added or AsA-added SLD imprinted biomaterial films. The reason can be explained by effects of function groups of plasticizers. That is, when CA with carboxyl and hydroxyl groups is added as a plasticizer, cavities that can adsorb a lot of SLD as target drug can be formed by combinations among MBS, PVA, CA, and SLD. In addition, the adsorption of SLD on SLD imprinted biomaterial films added with AsA having hydroxyl and ketone groups is higher than that of biomaterial films added with GL having only hydroxyl groups. These results can be verified by Scatchard plot analysis

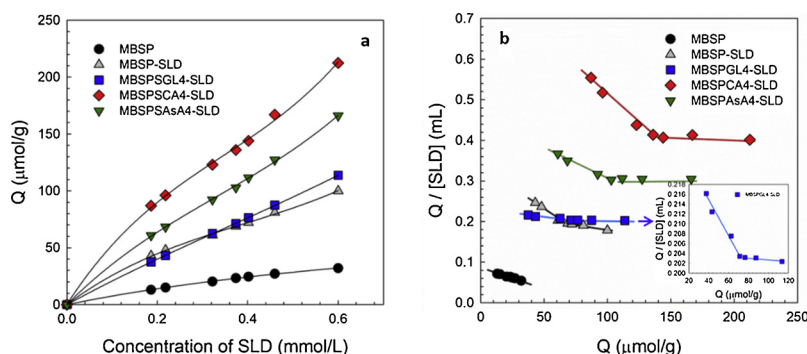


Fig. 5. Recognition properties of SLD imprinted MBS/PVA biomaterial films. (a) Binding isotherm of SLD imprinted MBS/PVA biomaterial films. (b) Scatchard plot analysis of SLD imprinted MBS/PVA biomaterial films.

which can provide binding site and affinity of the target molecule. Calculated binding isotherm data was plotted using Scatchard Eq. (5). Results showed two distinct sections within the plot that could be regarded as straight lines (Fig. 5b). These two lines indicate that there are two classes of binding sites in SLD imprinted biomaterial films. However, in case of non-imprinted biomaterial films, the adsorption classification had only one straight line. The steep line and flat line are related to high affinity sites as specific binding sites and low affinity sites as non-specific binding sites, respectively (Liu et al., 2016). Thus, Eq. (5) can be rewritten as follows:

$$Q / [Template] = \frac{(Q_{\max 1} - Q_1)}{K_{D1}} + \frac{(Q_{\max 2} - Q_2)}{K_{D2}} \quad (6)$$

where Q is the adsorbed amount of SLD bound to SLD imprinted biomaterial film at equilibrium, Q_{\max} is the apparent maximum number of binding sites, $[Template]$ is the free concentration of SLD at equilibrium and K_D is the equilibrium dissociation constant of binding sites. In addition, Q_1 , $Q_{\max 1}$, and K_{D1} describe high affinity sites while Q_2 , $Q_{\max 2}$, and K_{D2} explain low affinity sites.

Table 3 shows results of equilibrium dissociation constants (K_D , K_{D1} , and K_{D2}) and apparent maximum numbers (Q_{\max} , $Q_{\max 1}$, and $Q_{\max 2}$) calculated by Eq. (6). According to results, values of K_D and Q_{\max} demonstrated that the prepared SLD imprinted biomaterial films had good binding ability and adsorption capacity. Additionally, when K_D values of SLD imprinted biomaterial films prepared with different types of plasticizers (GL, CA, and AsA) were compared, CA-added SLD imprinted biomaterial films had lower values than GL-added or AsA-added SLD imprinted biomaterial films. Generally, the lower the K_D value, the higher the binding affinity (Liu, An, Ren, Feng, & Ma, 2018). These results indicate that the recognition ability of CA-added SLD imprinted biomaterial films is superior to that of others.

3.4. Release properties for SLD *in vitro*

Release property of SLD as a target drug in transdermal drug delivery system (TDDS) was determined *in vitro*. Fig. 6 shows results of SLD release ratio (%) on the prepared biomaterial films and SB and S for non-imprinted biomaterial films with the change of pH and temperature. To verify the effects of pH and temperature of non-imprinted biomaterial films, we investigated SB and S values with the change of

pH and temperature. The results indicated that SB and S had similar values with the change of pH, although they were a slight difference in the increase of temperature. From the results, it can be known that the change of pH has little effect on biomaterial films networks. Results of release ratio (%) of SLD for SLD imprinted biomaterial films without addition of plasticizer at different pH and temperature conditions are shown in Fig. 6a–c. Cumulative amount of SLD released from these films was more than about 95.0% within 10 h. In addition, SLD release at pH 10 and 45 °C was superior to that at pH 4 and 25 °C. The reason is related to the solubility of SLD with the change of pH. Sánchez-González, Yépez-Mulia, Hernández-Abad, and Cook, (2015) have reported that the solubility of SLD increased with the increase of pH. Thus, it could be confirmed that SLD release on SLD imprinted biomaterial films at high pH ranges was more than that at low pH ranges.

The release profile of SLD using human skin (pH 6.8 and 36.5 °C) is shown in Fig. 6d. Results showed that SLD imprinted in biomaterial films was released rapidly with an increase in time of release (within 10 h). There was difference in the degree of SLD release depending on with the type of plasticizers added. The degree of release for SLD had the following decreasing order: MBSP-SLD > MBSPGL4-SLD > MBSPAsA4-SLD > MBSPCA4-SLD. A possible explanation for this result could be related to the effect of functional groups of CA used as plasticizer. This result suggests that the degree of release for SLD as a target drug can be controlled by the type of plasticizer. However, drug release was relatively fast because the release condition was in aqueous solution. Therefore, SLD release experiment was performed using artificial skin to evaluate the possibility of application as a TDDS patch.

Fig. 7 represents SLD release ratio (%) on SLD imprinted biomaterial films using artificial skin. Results showed that cumulative release rate of SLD from SLD imprinted biomaterial films was increased at a relatively steady rate with increasing time. The cumulative release amount was about 95.0–98.0% for 24 days. There was also difference in the degree of release depending on the type of plasticizer. These results confirmed that the prepared drug imprinted biomaterial films could be applied as TDDS patch.

4. Conclusions

Sulindac (SLD) imprinted biomaterial films using MBS, PVA, and plasticizers (GL, CA, and AsA) were successfully prepared by UV

Table 3

K_{D1} and Q_{\max} to be calculated from the slope and intercept of the Scatchard plot.

Sample name	K_{D1} ($\mu\text{mol/g}$)	K_{D2} ($\mu\text{mol/g}$)	K_D ($\mu\text{mol/g}$)	$Q_{\max 1}$ ($\mu\text{mol/L}$)	$Q_{\max 2}$ ($\mu\text{mol/L}$)	Q_{\max} ($\mu\text{mol/L}$)
MBSP-SLD	476.19	1666.67	2142.86	159.24	390.17	549.41
MBSPGL4-SLD	3333.33	49998.8	53332.13	761.33	10248.5	11009.83
MBSPCA4-SLD	344.83	1666.67	2011.50	275.35	814.84	1090.19
MBSPAsA4-SLD	666.67	3333.33	4000.00	303.21	1125.67	1428.88

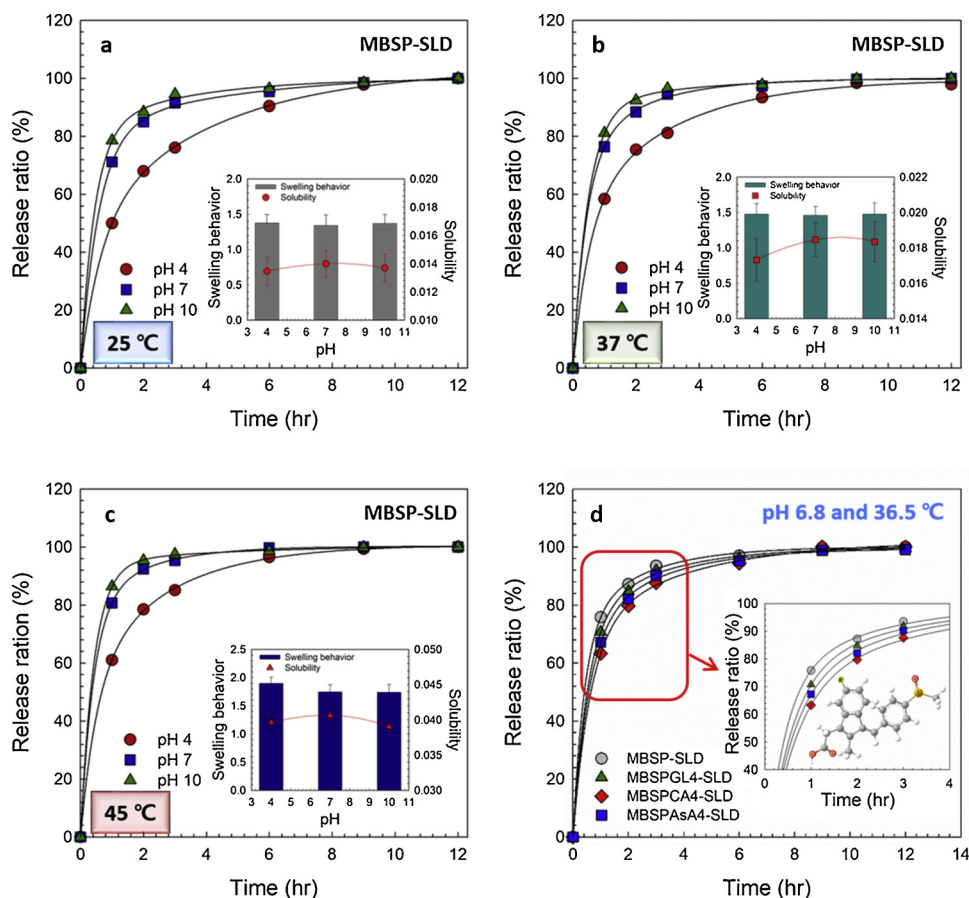


Fig. 6. SLD release ratio (%) on SLD imprinted biomaterial films and swelling behavior and solubility for non-imprinted biomaterial films with the change of pH and temperature. (a) SLD release ratio (%) on the prepared biomaterial films without addition of plasticizer with changes of pH at 25 °C. (b) SLD release ratio (%) on the prepared biomaterial films without addition of plasticizer with changes of pH at 37 °C. (c) SLD release ratio (%) on the prepared biomaterial films without addition of plasticizer with changes of pH at 45 °C. (d) SLD release ratio (%) on the prepared biomaterial films with addition of plasticizers at pH 6.8 and 37 °C.

irradiation process and casting methods. In order to optimize UV irradiation time for the preparation of SLD imprinted biomaterial films, physical properties such as tensile strength (TS), elongation at break (% E), swelling behavior (SB), and solubility (S), gel fraction, and FT-IR analysis were investigated with different UV irradiation time. The results indicated that the optimal UV irradiation time was about 30 min. These prepared SLD imprinted biomaterials films were then characterized by SEM analysis. In addition, physical properties and functionality such as recognition ability and applicability as transdermal drug delivery systems (TDDS) patch films were investigated. From the results of recognition ability, we revealed that the prepared SLD imprinted biomaterial films had high recognition abilities. To apply them as TDDS patch, we evaluated the SLD release ratio (%) for SLD imprinted biomaterial films at different pH and temperature conditions.

Results indicated that SLD release at pH 10.0 and 45 °C was more than that at pH 4.0 and 25 °C. In addition, the release rate of SLD was examined using artificial skin. Results revealed that SLD cumulative release rate from SLD imprinted biomaterial films was increased at a relatively steady rate for 20 days. These results indicate that they can be applied in medical patches and various fields.

Acknowledgments

This research was supported by Jeonnam Green Environment Center (JNGEC, South Korea) (Grant no. JNGEC/R-17-3-10-16-9).

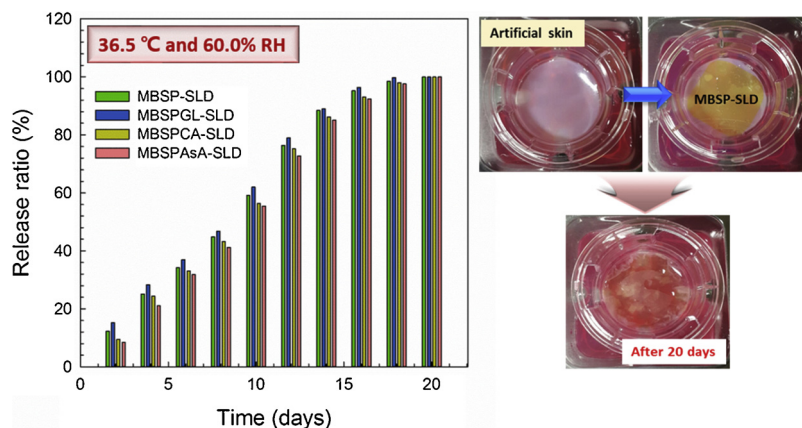


Fig. 7. SLD release ratio (%) on SLD imprinted MBS/PVA biomaterial films using artificial skin at 36.5 °C and 60.0% RH.

References

- Ali, A., Xie, F., Yu, L., Liu, H., Meng, L., Khalid, S., et al. (2018). Preparation and characterization of starch-based composite films reinforced by polysaccharide-based crystals. *Composites Part B Engineering*, *133*, 122–128.
- Asbill, C., Kim, N., El-Kattan, A., Creek, K., Wertz, P., & Michniak, B. (2000). Evaluation of a human bio-engineered skin equivalent for drug permeation studies. *Pharmaceutical Research*, *17*, 1092–1097.
- Aydn, A. A., & Ilberg, V. (2016). Effect of different polyol-based plasticizers on thermal properties of poly(vinyl alcohol): Starch blends. *Carbohydrate Polymers*, *136*, 441–448.
- Banerjee, S., Chattopadhyay, P., Ghosh, A., Datta, P., & Veer, V. (2014). Aspect of adhesives in transdermal drug delivery systems. *International Journal of Adhesion & Adhesives*, *50*, 70–84.
- Brown, M. B., Martin, G. P., Jones, S. A., & Akomeah, F. K. (2006). Dermal and transdermal drug delivery systems: Current and future prospects. *Drug Delivery*, *13*, 175–187.
- Byun, H. S., Park, M. H., Lim, G. T., & Yoon, S. D. (2011). Physical properties and characterization of biodegradable films using nano-sized TiO₂/poly(acrylamide-co-methylmethacrylate) composite. *Journal of Nanoscience and Nanotechnology*, *11*, 1701–1705.
- Cieřla, K., Abramowska, A., Boguski, J., & Drewnik, J. (2017). The effect of poly(vinyl alcohol) type and radiation treatment on the properties of starch-poly(vinyl alcohol) films. *Radiation Physics and Chemistry*, *141*, 142–148.
- Das, K., Ray, D., Bandyopadhyay, N. R., Gupta, A., Sengupta, S., Sahoo, S., et al. (2010). Preparation and characterization of cross-linked starch/poly(vinyl alcohol) green films with low moisture absorption. *Industrial & Engineering Chemistry Research*, *49*, 2176–2185.
- Delville, J., Joly, C., Dole, P., & Bliard, C. (2002). Solid state photocrosslinked starch based films: A new family of homogeneous modified starches. *Carbohydrate Polymers*, *49*, 71–81.
- Elizondo, N. J., Sobral, P. J. A., & Menegalli, F. C. (2009). Development of films based on blends of Amaranthus cruentus flour and poly(vinyl alcohol). *Carbohydrate Polymers*, *75*, 592–598.
- Follain, N., Joly, C., Dole, P., & Bliard, C. (2005). Properties of starch based blends. Part 2. Influence of poly(vinyl alcohol) addition and photocrosslinking on starch based materials mechanical properties. *Carbohydrate Polymers*, *60*, 185–192.
- Fu, L., Zhu, J., Zhang, S., Li, X., Zhang, B., Pu, H., et al. (2018). Hierarchical structure and thermal behavior of hydrophobic starch-based films with different amylose contents. *Carbohydrate Polymers*, *181*, 528–535.
- Imre, B., & Pukánszky, B. (2013). Compatibilization in bio-based and biodegradable polymer blends. *European Polymer Journal*, *49*, 1215–1233.
- Jose, J., Al-Harthi, M. A., AlMáadeed, M. A. A., Dakua, J. B., & De, S. K. (2015). Effect of graphene loading on thermomechanical properties of poly(vinyl alcohol)/starch blend. *Journal of Applied Polymer Science*, *132*, 41827–41834.
- Kim, D. S., Park, B. H., Rhim, J. W., & Lee, Y. M. (2005). Proton conductivity and methanol transport behavior of cross-linked PVA/PAA/silica hybrid membranes. *Solid State Ionics*, *176*, 117–126.
- Kwak, M. K., Jeong, H. E., & Suh, K. Y. (2011). Rational design and enhanced biocompatibility of a dry adhesive medical skin patch. *Advanced Materials*, *23*, 3949–3953.
- Lam, P. L., & Gambari, R. (2014). Advanced progress of microencapsulation technologies: In vivo and in vitro models for studying oral and transdermal drug deliveries. *Journal of Controlled Release*, *178*, 25–45.
- Liu, P., An, H., Ren, Y., Feng, J., & Ma, J. (2018). Selective recognition mechanism of molybdenum(VI) ions binding onto ion imprinted particle in the water. *Chemical Engineering Journal*, *349*, 176–183.
- Liu, X., Zhu, L. I., Gao, X., Wang, Y., Lu, H., Tang, Y., et al. (2016). Magnetic molecularly imprinted polymers for spectrophotometric quantification of curcumin in food. *Food Chemistry*, *202*, 309–315.
- Liu, Z., Dong, Y., Men, H., Jiang, M., Tonga, J., & Zhou, J. (2012). Post-crosslinking modification of thermoplastic starch/PVA blend films by using sodium hexametaphosphate. *Carbohydrate Polymers*, *89*, 473–477.
- Lv, D., Zhu, M., Jiang, Z., Jiang, S., Zhang, Q., & Xiong, R. (2018). Green electrospun nanofibers and their application in air filtration. *Macromolecular Materials and Engineering*, *303*, 1800336–1800353.
- Ma, X., Chang, P. R., Yu, J., & Lu, P. (2008). Electrically conductive carbon black (CB)/glycerol plasticized-starch (GPS) composites prepared by microwave radiation. *Starch-Starke*, *60*, 373–375.
- Maciążek-Jurczyk, M., & Sułkowska, A. (2015). Spectroscopic analysis of the impact of oxidative stress on the structure of human serum albumin (HSA) in terms of its binding properties. *Spectrochimica Acta Part A, Molecular and Biomolecular Spectroscopy*, *136*, 265–282.
- Mikus, P. Y., Alix, S., Soulestin, J., Lacrampe, M. F., Krawczak, P., Coqueret, X., et al. (2014). Deformation mechanisms of plasticized starch materials. *Carbohydrate Polymers*, *114*, 450–457.
- Nair, L. S., & Laurencin, C. T. (2007). Biodegradable polymers as biomaterials. *Progress in Polymer Science*, *32*, 762–798.
- Niazi, M. B. K., & Broekhuis, A. A. (2015). Surface photo-crosslinking of plasticized thermoplastic starch films. *European Polymer Journal*, *64*, 229–243.
- Noori, S., Kokabi, M., & Hassan, Z. M. (2018). Poly(vinyl alcohol)/chitosan/honey/clay responsive nanocomposite hydrogel wound dressing. *Journal of Applied Polymer Science*, *135*, 46311–46322.
- Prausnitz, M. R., & Langer, R. (2008). Transdermal drug delivery. *Nature Biotechnology*, *26*, 1261–1268.
- Reddy, N., & Yang, Y. (2010). Citric acid cross-linking of starch films. *Food Chemistry*, *118*, 702–711.
- Robles, E., Salaberria, A. M., Herrera, R., Fernandes, S. C., & Labidi, J. (2016). Self-bonded composite films based on cellulose nanofibers and chitin nanocrystals as antifungal materials. *Carbohydrate Polymers*, *144*, 41–50.
- Sadanand, V., Rajini, N., Rajulu, A. V., & Satyanarayana, B. (2016). Preparation of cellulose composites with *in situ* generated copper nanoparticles using leaf extract and their properties. *Carbohydrate Polymers*, *150*, 32–39.
- Sánchez-González, E. G., Yépez-Mulia, L., Hernández-Abad, V. J., & Cook, H. J. (2015). The influence of polymorphism on the manufacturability and *in vitro* dissolution of sulindac-containing hard gelatin capsules. *Pharmaceutical Development and Technology*, *20*, 306–313.
- Sanuja, S., Agalya, A., & Umapathy, M. J. (2015). Synthesis and characterization of zinc oxide-neem oil-chitosan bionanocomposite for food packaging application. *International Journal of Biological Macromolecules*, *74*, 76–84.
- Tian, H., Tang, Z., Zhuang, X., Chen, X., & Jing, X. (2012). Biodegradable synthetic polymers: Preparation, functionalization and biomedical application. *Progress in Polymer Science*, *37*, 237–280.
- Tian, H., Yan, J., Rajulu, A. V., Xiang, A., & Luo, X. (2017). Fabrication and properties of poly(vinyl alcohol)/starch blend films: Effect of composition and humidity. *International Journal of Biological Macromolecules*, *96*, 518–523.
- Wang, Y. F., Liu, H. S., Xie, F. W., Yu, L., Zhang, L., Liao, L., et al. (2016). Morphology and properties of thermal/cooling-gel bi-phasic systems based on hydroxypropyl methylcellulose and hydroxypropyl starch. *Composites Part B Engineering*, *101*, 46–52.
- Wu, Y. H., Luo, X. G., Li, W., Song, R., Li, J., Li, Y., et al. (2016). Green and biodegradable composite films with novel antimicrobial performance based on cellulose. *Food Chemistry*, *197*, 250–256.
- Xiao, X., & Hao, C. (2010). Preparation of waterborne epoxy acrylate/silica sol hybrid materials and study of their UV curing behavior. *Colloids and Surfaces A, Physicochemical and Engineering Aspects*, *359*, 82–87.
- Xie, F., Pollet, E., Halley, P. J., & Avérous, L. (2013). Starch-based nano-biocomposites. *Progress in Polymer Science*, *38*, 1590–1628.
- Yu, C., Tang, X., Liu, S., Yang, Y., Shen, X., & Gao, C. (2018). Laponite crosslinked starch/poly(vinyl alcohol) hydrogels by freezing/thawing process and studying their cadmium ion absorption. *International Journal of Biological Macromolecules*, *117*(2018), 1–6.
- Yu, L., Dean, K., & Li, L. (2006). Polymer blends and composites from renewable resources. *Progress in Polymer Science*, *31*, 576–602.
- Yun, Y. H., & Yoon, S. D. (2010). Effect of amylose contents of starches on physical properties and biodegradability of starch/PVA-blended films. *Polymer Bulletin*, *64*, 553–568.
- Yun, Y. H., Lee, C. M., Kim, Y. S., & Yoon, S. D. (2017). Preparation of chitosan/poly(vinyl alcohol) blended films containing sulfosuccinic acid as the crosslinking agent using UV curing process. *Food Research International*, *100*, 377–386.
- Zhai, M., Yoshii, F., & Kume, T. (2003). Radiation modification of starch-based plastic sheets. *Carbohydrate Polymers*, *52*, 311–317.
- Zhang, J. Y., Windall, G., & Boyd, I. W. (2002). UV curing of optical fibre coatings using excimer lamps. *Applied Surface Science*, *186*, 568–572.
- Zhou, J., Ma, Y., Ren, L., Tong, J., Liu, Z., & Xie, L. (2009). Preparation and characterization of surface crosslinked TPS/PVA blend films. *Carbohydrate Polymers*, *76*, 632–638.